

# A Sudden-Release Bristle Model that Exhibits Hysteresis and Stick-Slip Friction

Bojana Drinčić and Dennis S. Bernstein

**Abstract**—In this paper we introduce a bristle model for stick-slip friction. The friction force of the bristle model is generated by frictionless contact between a body and an infinite row of bristles. Each bristle is attached to the ground through a torsional spring so that, as the body moves, the bristles pivot and counteract its motion. We show that the bristle model exhibits stick-slip motion similar to that of the LuGre model. We then form a hybrid model by combining the LuGre and bristle models.

## I. INTRODUCTION

Friction is a singular problem in its impact on real-world systems. Excessive friction contributes to wasted energy measured in billions of dollars, whereas insufficient friction contributes to accidents and damage. In manufacturing applications, friction is crucial to grinding and polishing, and it is a limiting factor in achieving precision motion control. In scientific applications, such as atomic force microscopes and nano-scale devices, friction plays a crucial role.

From a scientific point of view, friction is extremely difficult to model from first principles. Contributing factors include the molecular properties and geometry of the contacting surfaces, as well as fluid-structure interaction when lubricants are present. Friction can be viewed as a macro-scale phenomenon that emerges from a large-scale system of interacting components.

In control applications, various empirical models have been developed to capture the key features of friction [1–4]. These models can be fit to data to capture the characteristics of a specific application, or they can be used as the basis of adaptive control techniques in which parameters are identified and controller gains are adapted during operation [5–8].

In the present paper we focus on stick-slip friction, which refers to motion in which friction causes a body attached by a compliance to periodically and momentarily come to rest. This kind of motion, which is reminiscent of a limit cycle, occurs when the friction has specific characteristics near zero velocity; the LuGre model can reproduce stick-slip friction, as can other friction models [4, 9–15].

In the present paper we take a fundamental approach to modeling friction by using a bristle model, which can be viewed as an asperity model with rigid asperities [16–18]. The unconventional aspect of the bristle model in the present paper is that the interactions between the bristles and the

contacting body are frictionless. Our goal is thus to discover how friction can emerge from a model that is frictionless and contact that is lossless.

The clue to constructing a hysteretic dissipation mechanism for friction without introducing friction per se is to recognize that hysteresis is a quasi-DC phenomenon, which means that energy dissipation must occur under asymptotically slow motion. In fact, friction is closely related to hysteresis in the sense that energy is dissipated during cyclical motion under arbitrarily slow motion [19].

To capture this idea within a bristle model, we assume that each bristle has a torsional spring at its base. As a moving body comes into contact with each bristle, reaction forces occur, but otherwise the contact is lossless and thus frictionless. As the moving body passes over a bristle, the bristle is released, and its subsequent motion causes a minimal level of energy dissipation regardless of how slowly the mass moves. The resulting force model is thus hysteretic.

In the present paper we combine the bristle model with a compliance in order to determine whether stick-slip motion can occur. The simulation in Section III shows that stick-slip friction occurs when the body is attached to a wall through a spring and driven by a periodic force. Furthermore, the input-output map in this scenario is hysteretic, and the area of the hysteresis map is equal to the energy expended to pivot the bristles. Simulations of the body attached to a spring whose free end moves at a constant velocity show the existence of a stable stick-slip limit cycle, similar to the limit cycles of the LuGre model. In Section IV we form a hybrid model for stick-slip by combining the LuGre and bristle models.

## II. BRISTLE MODEL

The friction force of the bristle model is generated through the frictionless interaction between a body and bristles as shown in Figure 1. The body of mass  $m$  and length  $w$  moves over an infinite row of rigid bristles, each of which has length  $l_S$ . At the base of each bristle is a torsional spring with stiffness coefficient  $\kappa$ . The distance between the bristles is  $\Delta$ , and the position the  $i$ th bristle is denoted by  $x_{b_i}$ . As the body moves, there is a force at the point of contact between the bristle and the body. The force is due to the torsional spring at the base of each bristle. We assume that the contact is frictionless and the force on the body is perpendicular to the direction of the bristle, so that only the horizontal component of the contact force contributes to the friction. The sum of all horizontal forces exerted by the bristles that are touching the body at any instant is the friction force.

This work was supported in part by the National Defense Science and Engineering Graduate Fellowship.

The authors are with the Department of Aerospace Engineering, The University of Michigan, Ann Arbor, MI 48109-2140. bojanad@umich.edu

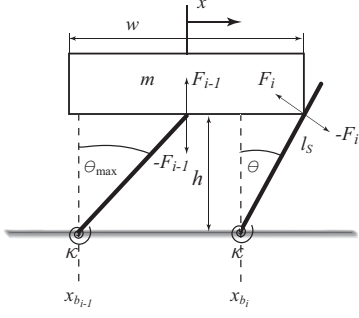


Fig. 1. Schematic representation of the body and bristle contact. The body has mass  $m$  and width  $w$ . The bristle has length  $l_S$ . At the base of each bristle is a torsional spring with stiffness  $\kappa$ .

We use the vertical force equilibrium and geometry to find the maximum angle  $\theta_{\max}$  that a bristle can pivot. Note that the contact between the body and the bristle is frictionless, and thus the horizontal component of the contact force drops discontinuously to zero at the moment when the angle of the bristle deflection becomes  $\theta_{\max}$ . We assume that there are  $N$  bristles in contact with body of length  $w$  so that  $N - 1 = w/\Delta$  and that the mass moves only horizontally. We start with Hooke's law for a torsional spring and assume that  $N$  bristles under the body are pivoted by  $\theta_{\max}$ . Then the moment in each of the springs attached to these bristles is  $\tau_i = \kappa\theta_{\max} = F_i l_S$ , so that the sum of the forces in the vertical direction is

$$N F_i - mg = N \frac{\kappa\theta_{\max}}{l_S} - mg = 0, \quad (1)$$

where  $g$  is the acceleration due to gravity. The maximum angle of deflection is therefore

$$\theta_{\max} = \frac{mgl_S}{N\kappa}, \quad (2)$$

where  $\theta_{\max} < \frac{\pi}{2}$  and the height from the base of the bristles to the body is  $h = l_S \cos(\theta_{\max})$ .

If the  $i$ th bristle is pivoted less than  $\theta_{\max}$ , then its angle of rotation  $\theta_i$  can be found from geometry. If the body is moving to the right, that is,  $\dot{x} \geq 0$ , then the angle of rotation of a bristle is given by

$$\theta_i = \tan^{-1} \left( \frac{x + \frac{w}{2} - x_{b_i}}{h} \right), \quad (3)$$

whereas, if the body is moving to the left, then

$$\theta_i = \tan^{-1} \left( \frac{x - \frac{w}{2} - x_{b_i}}{h} \right). \quad (4)$$

Because the contact between the body and the bristles is frictionless, once the bristle reaches the maximum angle of deflection, the force contribution from that bristle drops to zero. Thus, the friction force is equal to the sum of the forces exerted by each bristle in contact with the body and pivoted less than  $\theta_{\max}$ . The distance from the base of the  $i$ th bristle

to the point at which the force acts is  $r_i = \frac{h}{\cos \theta_i}$ , and the total force applied to  $i$ th bristle is  $F_i = \frac{\kappa\theta_i}{r_i}$ . The total friction force is thus

$$F_f = \sum_{i=1}^n F_i \cos \theta_i = \sum_{i=1}^n \frac{\kappa\theta_i (\cos \theta_i)^2}{h}, \quad (5)$$

where  $n$  is the number of bristles that are in contact with the body and that are bent less than  $\theta_{\max}$ .

Which bristles are in contact with the body can be determined based on the position of the bristles relative to the body. If the body is moving to the right, then bristles are pivoted at an angle determined by (3) if  $x_{b_i}$  satisfies

$$x + \frac{w}{2} - d < x_{b_i} \leq x + \frac{w}{2}, \quad (6)$$

where  $d \triangleq \sqrt{l_S^2 - h^2}$ . If the body is moving to the left, then the bristles are pivoted at an angle determined from (4) if

$$x - \frac{w}{2} < x_{b_i} \leq x - \frac{w}{2} + d. \quad (7)$$

### III. ANALYSIS OF THE BRISTLE MODEL

In order to test the input-output and stick-slip properties of the bristle model we consider the two body-spring configurations shown in Figure 2. In Figure 2(a) the body of mass  $m$  is connected to a wall by means of a spring with stiffness  $K$  and is acted on by the force input  $u$ . The equation of motion is

$$\begin{aligned} \dot{x} &= v, \\ \dot{v} &= \frac{1}{m}(-Kx + u - F_f), \end{aligned} \quad (8)$$

where  $x$  is the position of the center of mass of the body,  $u$  is the force input, and  $F_f$  is the friction force. In Figure 2(b) the body of mass  $m$  is connected to a spring with stiffness  $K$ . The free end of the spring moves at the constant speed  $v_p$ . The equations of motion are

$$\begin{aligned} \dot{x} &= v, \\ \dot{v} &= \frac{1}{m}(Kl - F_f), \\ \dot{l} &= v_p - v, \end{aligned} \quad (9)$$

where  $l$  is the length of the spring and  $F_f$  is the friction force.

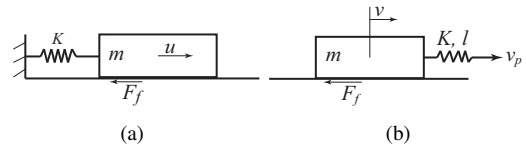


Fig. 2. The two configurations used to test the bristle model. In (a) the body of mass  $m$  is connected to the wall by a means of a spring with stiffness  $K$  and is acted on by the force input  $u$ . In configuration shown in (b) the body of mass  $m$  is connected to a spring with stiffness  $K$ . The free end of the spring moves at the constant speed  $v_p$ .

### A. Hysteresis map

We simulate the system in Figure 2(a) with a sinusoidal force input,  $u(t) = \sin(\omega t)$  N, in order to obtain the input-output map for the bristle model. We vary the frequency of the input to show that the output of the system is rate dependent. The friction force  $F_f$  is obtained from (5). The input-output maps of (8) with  $\omega = 0.05$  rad/s is shown in Figure 3(a). The input-output map with  $\omega = 0.001$  rad/s is shown in Figure 3(b). Note that the input-output map at low frequency is hysteretic and has a staircase shape typical for stick-slip. The time histories of  $x$ ,  $\dot{x}$ ,  $u$ , and  $F_f$  are shown in Figure 3(c).

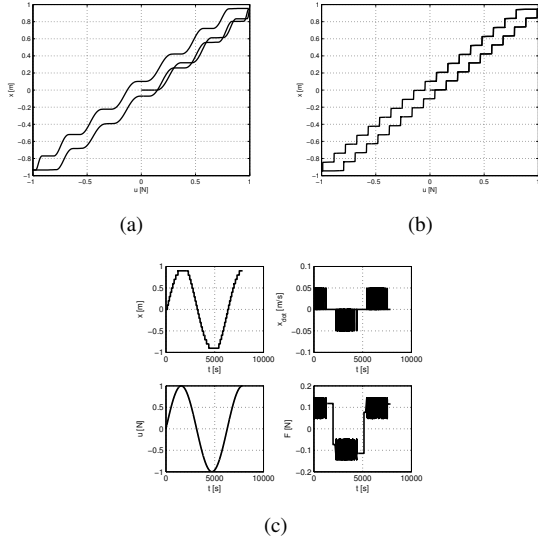


Fig. 3. Simulation of system (8)  $u(t) = \sin(\omega t)$  N, with  $l_S = 0.1$  m,  $\kappa = 0.1$  N-m/rad,  $m = 1$  kg,  $K = 1$  N/m,  $w = 1$  m,  $N = 101$  and  $\Delta = w/(N - 1)$  m. (a) shows the input-output map with  $\omega = 0.05$  rad/s and (b) shows the input-output map with  $\omega = 0.001$  rad/s. The shape of the input-output map at low frequency is typical of stick-slip. Time histories of  $x$ ,  $v$ ,  $u$  and  $F_f$  with  $\omega = 0.001$  rad/s are shown in (c).

### B. Energy Calculation

Since the input-output map of (8) is hysteretic, we can calculate the energy dissipated during one cycle of operation. The area of the hysteresis map shown in Figure 3(b) is equal to the energy loss during one cycle. Alternatively, we can calculate the dissipated energy by summing the potential energy stored in each torsional spring during the motion of the body. Note that the mass and inertia of each bristle are irrelevant to the amount of dissipated energy. Assuming that the angle of each bristle that the body contacts reaches  $\theta_{\max}$ , the total energy loss is

$$E_{\text{stored}} = \frac{1}{2} M \kappa \theta_{\max}^2, \quad (10)$$

where  $M$  is the number of bristles that the mass contacts during one cycle. Based on the minimum and maximum value of  $x$  during one cycle and the spacing of the bristles,

$M$  is given by

$$M = \frac{x_{\max} - x_{\min}}{\Delta}. \quad (11)$$

The energy dissipated based on the area of the hysteresis loop shown in Figure 3(b) is  $E = 0.35647$  J, while the energy calculated from (10) is  $E_{\text{stored}} = 0.35566$  J.

### C. Approximation of the friction force

The calculation of the friction force requires keeping track of the position of each bristle relative to the mass. In order to make this process easier we note that the friction force of the bristle model is a function of position that closely resembles a sawtooth wave as shown in Figure 4(a). Thus, the friction force can be approximated by a sawtooth wave, so that (5) is replaced by

$$F_f \approx \text{sign}(v) \left( F_l + \frac{F_h - F_l}{\Delta} \text{mod}(\text{sign}(v)x, \Delta) \right), \quad (12)$$

where  $F_l$  and  $F_h$  are constants that determine the magnitude of the friction force. The force  $F_f$  given by (12) is shown in Figure 4(b). This approximation is useful because the force depends only on the current position of the body and the spacing between the bristles.

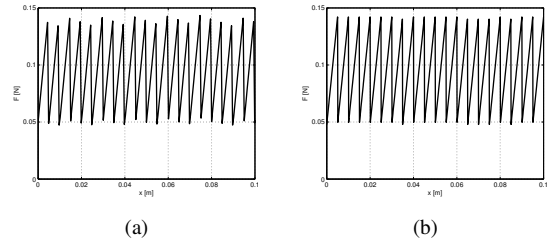


Fig. 4. The friction force as a function of position. (a) shows the friction force obtained from (5) with  $N = 101$ ,  $\Delta = 0.005$  m,  $m = 1$ ,  $l_S = 0.1$  m,  $\kappa = 0.1$  N-m/rad,  $w = 0.5$  m. (b) shows the approximation (12) of the friction force with  $F_l = 0.14$  N,  $F_h = 0.05$  N,  $\Delta = 0.005$ .

### D. Equilibria

In this section we define the equilibria of the system for a constant value of the input, that is, for  $u(t) = \bar{u}$ . Due to discontinuities in the system for  $v = 0$  and  $x = k\Delta$ , where  $k \in \mathbb{N}$ , we use discontinuous system theory to analyze the equilibria of the system (see [20]). We note that  $v = 0$  is a sliding manifold of the system and also that  $\dot{x} = 0$  implies  $v = 0$ . Thus we look for equilibria on the sliding manifold  $v = 0$ . On this sliding manifold, we redefine the dynamics as follows

$$\begin{bmatrix} \dot{x} \\ \dot{v} \end{bmatrix} = \alpha f_+ + (1 - \alpha) f_-, \quad \alpha \in [0, 1], \quad (13)$$

where

$$f_+ = \begin{bmatrix} v \\ \frac{1}{m}(-Kx + u - F_{f+}) \end{bmatrix}, \quad (14)$$

$$f_- = \begin{bmatrix} v \\ \frac{1}{m}(-Kx + u - F_{f-}) \end{bmatrix}, \quad (15)$$

and

$$F_{f+} = Fl + \frac{Fh - Fl}{\Delta} \text{mod}(x, \Delta), \quad (16)$$

$$F_{f-} = -(Fl + \frac{Fh - Fl}{\Delta} \text{mod}(-x, \Delta)), \quad (17)$$

where on the sliding manifolds  $x = k\Delta$ , we re-define the function  $\text{mod}$  as a set-valued function, so that  $\text{mod}(k\Delta, \Delta) = [0, \Delta]$ . And thus, for  $v = 0$ , the set of equilibria is defined by

$$\mathcal{E} = \{(\bar{u}, x) : \bar{u} \in \mathbb{R}, x = \frac{\bar{u} - (\alpha F_{f+} + (1 - \alpha) F_{f-})}{K}, \alpha \in [0, 1]\}, \quad (18)$$

which is shown shaded in Figure 5. The hysteresis map is also shown in Figure 5. As expected, the hysteresis map is a subset of the equilibria map since the hysteresis map is obtained in the limit as the frequency of input goes to zero.

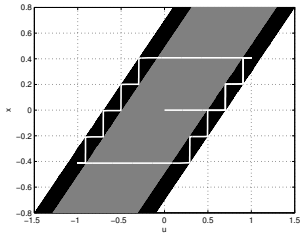


Fig. 5. Equilibria and hysteresis maps of the bristle model. The shaded area represents the equilibria of the system. The black portions represent the sliding manifolds for  $x = k\Delta$ ,  $k \in \mathbb{N}$ . The hysteresis map is shown in white and is a subset of the equilibria map. The parameters used are  $\kappa = 0.1$  N-m/rad,  $m = 1$  kg,  $K = 1$  N/m,  $\Delta = 0.005$  m,  $F_l = 0.5$  N, and  $F_h = 0.7$  N.

### E. Stick-Slip

To further investigate the stick-slip behavior of the bristle model we simulate the system in (9) with  $F_f$  given by (12). The output with  $v_p = 0.05$  m/s is shown in Figure 6. Part (a) of Figure 6 is the stick-slip limit cycle obtained by projecting the trajectories onto the  $l$ - $v$  plane. Figure 6(b) shows the time histories of  $x$ ,  $l$ ,  $v$ , and  $F_f$ .

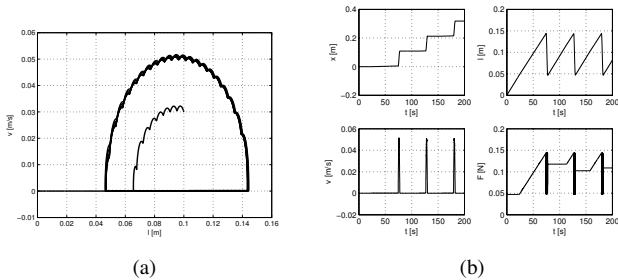


Fig. 6. The stick-slip limit cycle of the bristle model. (a) shows the stable limit cycle in the  $l$ - $v$  plane. The trajectories starting inside and outside of the limit cycle converge to it. (b) shows the time histories of  $x$ ,  $l$ ,  $v$ , and  $F_f$  with zero initial conditions. The parameter values are  $m = 1$  kg,  $K = 1$  N/m,  $v_p = 0.001$  m/s,  $F_h = 0.14$  N,  $F_l = 0.05$  N, and  $\Delta = 0.005$  m.

We now consider the same system with the friction force of the LuGre friction model [4]

$$\dot{q} = v - \frac{|v|}{r} q, \quad (19)$$

$$r = \frac{F_C}{\sigma_0} + \frac{F_S - F_C}{\sigma_0} e^{-(v/v_S)^2}, \quad (20)$$

$$F_{LG} = \sigma_0 q + \sigma_1 \dot{q} + \sigma_2 v, \quad (21)$$

where  $\sigma_0, \sigma_1, \sigma_2$  are constants,  $F_C$  is the Coulomb friction force,  $F_S$  is the stiction force, and  $v_S$  is the Stribeck velocity. The results of the simulation with  $v_p = 0.001$  m/s are shown in Figure 7, where (a) shows the stick-slip limit cycle in the  $l$ - $v$  plane and (b) shows the time histories of  $x$ ,  $v$ ,  $l$  and  $F_{LG}$ .

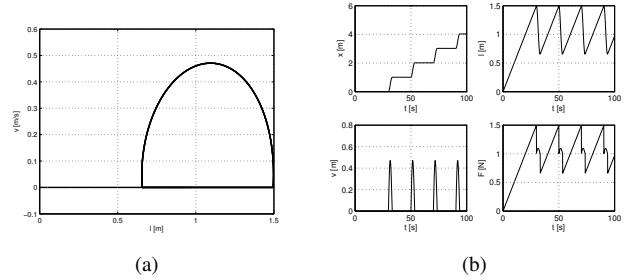


Fig. 7. The stick-slip limit cycle of the LuGre model with  $v_p = 0.05$  m/s. (a) shows the limit cycle in the  $l$ - $v$  plane. (b) shows the time histories of  $x$ ,  $l$ ,  $v$ ,  $F_{LG}$ . The parameter values are  $m = 1$  kg,  $K = 1$  N/m,  $\sigma_0 = 10^5$  N-s/m,  $\sigma_1 = \sqrt{10^5}$  N-s/m,  $\sigma_2 = 0.2$  N-s/m,  $v_s = 0.001$  m/s,  $F_C = 1$  N, and  $F_S = 1.5$  N.

Both models exhibit stick-slip motion as shown by the limit cycle in the  $l$ - $v$  plane. The limit cycle is characterized by a straight-line segment in which  $v = 0$  and  $\dot{l} = v_p$ . This straight-line segment represents the “stick” phase. The velocity of the body is zero, and the length of the spring increases at a steady rate. The body remains stationary until the spring is elongated so that the spring force becomes larger than the friction force. The body accelerates, and the length of the spring decreases. This is known as the “slip” phase. The spring is compressed until the spring force becomes smaller than the friction force and the mass becomes stationary. The mass sticks, and the process repeats.

## IV. HYBRID MODEL FOR STICK-SLIP FRICTION

Since the bristle model has several discontinuities, it is difficult to implement. We thus combine the bristle and LuGre models into a simplified version of the bristle model exhibiting stick-slip. We use geometry to find the derivative of the bristle-deflection angle  $\theta$  and combine it with the LuGre model.

We use the body-bristle geometry to find the time derivative of the bristle that is in contact with the front edge of the body. We assume that the spacing between the bristles is such that, at each moment, only one bristle is in contact with the front edge of the moving body. From the schematic

in Figure 8 we obtain

$$y = h \tan \theta, \quad (22)$$

where  $h = l_S \cos(\theta_{\max})$  is the height from the base of the bristles to the body and  $y$  is defined as in Figure 8. Since the mass and the bristle are in constant contact it follows that

$$\dot{y} = \dot{x} = v. \quad (23)$$

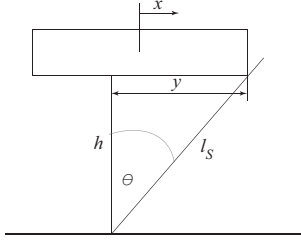


Fig. 8. Schematic representation of the bristle-mass contact. We assume that  $\Delta$  is large enough so that at each moment only one bristle is in contact with the front edge of the mass.

Combining (22) and (23) gives

$$\dot{y} = \dot{h} \tan \theta + \dot{\theta} h (\sec \theta)^2, \quad (24)$$

and since  $\dot{h} = 0$

$$\dot{\theta} = \frac{\dot{y}}{h (\sec \theta)^2} = \frac{v (\cos \theta)^2}{h}. \quad (25)$$

Equation (25) represents the motion of the bristle while  $\theta \leq \theta_{\max}$ . However (25) does not model the motion of the bristle once the angle reaches  $\theta_{\max}$  and a new bristle comes in contact with the front edge of the body. In order to account for these effects we augment (25) with a forgetting term adopted from the LuGre model. Equation (25) becomes

$$\dot{\theta} = \tilde{v} - \sigma \frac{|\tilde{v}|}{g(\tilde{v})} \theta, \quad (26)$$

$$\tilde{v} = \frac{v (\cos \theta)^2}{h}, \quad (27)$$

$$g(\tilde{v}) = \theta_1 + \theta_2 e^{-(\frac{\tilde{v}}{\epsilon})^2}, \quad (28)$$

where  $\sigma$ ,  $\epsilon$ ,  $\theta_1$ , and  $\theta_2$  are constants. To calculate the friction force due to the contact with the bristles we use (5). However, since we assumed that there is only one bristle in contact with the front end of the moving body (5) becomes

$$F_h = \frac{\sigma \kappa}{h} \theta (\cos \theta)^2. \quad (29)$$

We test the input-output properties of the hybrid model in the configuration shown in Figure 2(a). We use the equation of motion (8) with the friction force expressed by (26)-(29). The input-output map with  $u = 2 \sin(\omega t)$  N is shown in Figure 9. Figure 9(a) shows the input-output map for  $\omega = 0.1$  rad/s and Figure 9(b) shows the input-output map for  $\omega = 0.01$  rad/s. Since the input-output map is a non-trivial loop at low frequency it follows that that the system is hysteretic. The time histories of  $x$ ,  $v$ ,  $\theta$ , and  $F_h$  are shown in Figure 9(c). The parameter values used in the simulation are  $m = 1$

kg,  $K = 1$  N/m,  $\kappa = 10$  N-m/rad,  $h = 0.1$  m,  $\sigma = 10^3$  1/s,  $\theta_1 = 0.3$  rad,  $\theta_2 = 0.7$  rad, and  $\epsilon = 0.01$  1/s.

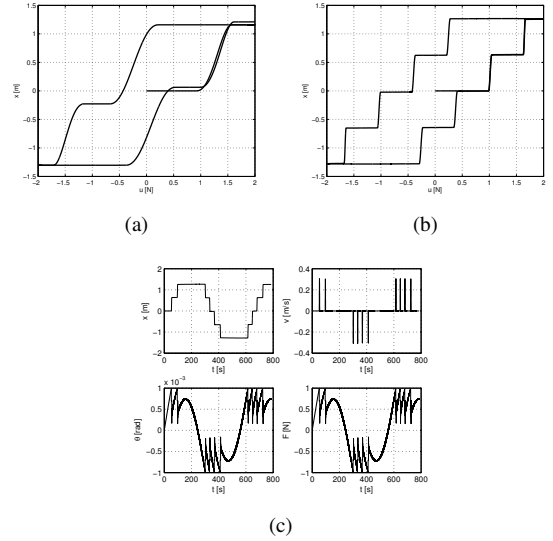


Fig. 9. Input-output maps of the hybrid model (26)-(29) with the input  $u = 2 \sin(\omega t)$  N. (a) shows the input-output map with  $\omega = 0.1$  rad/s. (b) shows the input-output map with  $\omega = 0.01$  rad/s. Note that the loop in the input-output map does not vanish at low frequency of excitation and thus the system is hysteretic. The time histories of  $x$ ,  $v$ ,  $\theta$ , and  $F_h$  at the lower frequency of excitation are shown in (c). The parameter values are  $m = 1$  kg,  $K = 1$  N/m,  $\kappa = 10$  N-m/rad,  $h = 0.1$  m,  $\sigma = 10^3$  1/s,  $\theta_1 = 0.3$  rad,  $\theta_2 = 0.7$  rad, and  $\epsilon = 0.01$  1/s.

To relate the hysteresis map to the equilibria map, we analyze the equilibria of this system for a constant value of the input,  $u = \bar{u}$ . The equilibria of (8) with friction force expressed by (26)-(29) are

$$\bar{x} = \frac{\bar{u} - F_h(\bar{\theta})}{K} \quad (30)$$

$$\bar{v} = 0 \quad (31)$$

$$\bar{\theta} = \text{sign}(0)g(0), \quad (32)$$

where  $\text{sign}(0) = [-1, 1]$ , so that (32) can be rewritten as

$$\bar{\theta} = (2\alpha - 1)g(0), \quad \alpha \in [0, 1]. \quad (33)$$

Thus, for each value of  $\bar{u}$  there is an infinite number of equilibria, and the equilibria map can be defined as

$$\mathcal{E} = \{(\bar{u}, x) : \bar{u} \in \mathbb{R}, x = \frac{\bar{u} - F_f(\bar{\theta})}{K}\}. \quad (34)$$

The equilibria map (34) and the hysteresis map are shown in Figure 10. The hysteresis map is a subset of the equilibria map.

We compare the output of the hybrid model to the output of the bristle model in the configuration shown in Figure 2(a). The outputs of both models are shown in Figure 11(a). The friction forces are compared in Figure 11(b). Except in the beginning, both friction forces follow the same pattern and are in the same range. Figure 11 demonstrates that both models can recreate the same stick-slip friction behavior.

To analyze the stick-slip limit cycle of the hybrid model

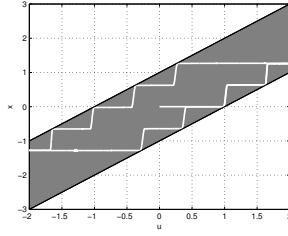


Fig. 10. Equilibria and hysteresis maps of the hybrid model. The shaded area represents the equilibria of the system. The hysteresis map is shown in white and is a subset of the equilibria map. The parameters used are  $\kappa = 10$  N-m/rad,  $m = 1$  kg,  $K = 1$  N/m,  $h = 0.1$  m,  $\sigma = 10^3$  1/s,  $\theta_1 = 0.3$  rad, and  $\theta_2 = 0.7$  rad.

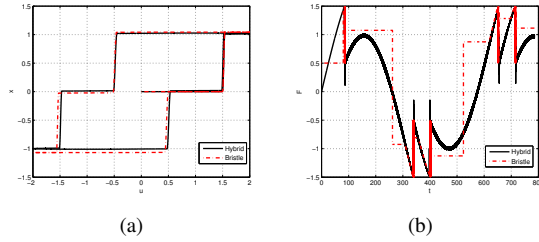


Fig. 11. Comparison of the outputs of the hybrid and bristle model. (a) shows the hysteresis maps in the configuration in Figure 2(a) while (b) compares the friction forces of the two models. The dashed line represents the bristle model and solid line shows the hybrid model. The hybrid model parameters are  $m = 1$  kg,  $K = 1$  N/m,  $\kappa = 10$  N-m/rad,  $h = 0.1$  m,  $\sigma = 10^3$  1/s,  $\theta_1 = 0.5$  rad,  $\theta_2 = 1$  rad, and  $\epsilon = 0.01$  1/s, and bristle model parameters are  $\Delta = 0.005$  m,  $F_l = 0.5$  N,  $F_h = 1.5$  N and the input is  $u = 2 \sin(0.01t)$ .

we simulate the friction model (26)-(29) in the body-spring configuration shown in Figure 2(b). The equations of motion are given by (9). The results of the simulation given in Figure 12(a) show a stick-slip limit cycle. The time histories of  $l$ ,  $v$ ,  $\theta$  and  $F_h$  are shown in Figure 12(b).

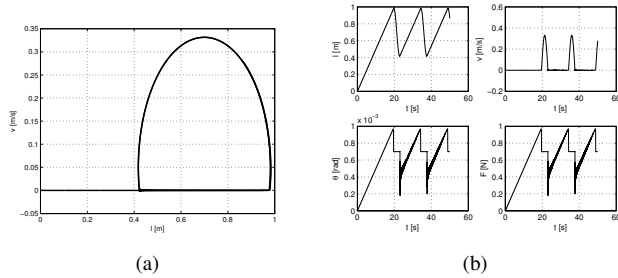


Fig. 12. The limit cycle of the system (26)-(29) with  $v_p = 0.05$  m/s. (a) shows the projection of the trajectory on the  $l$ - $v$  plane. The trajectory is a limit cycle with stick-slip. (b) shows the time history of  $l$ ,  $v$ ,  $\theta$ , and  $F_h$ . The parameter values are  $m = 1$  kg,  $K = 1$  N/m,  $\kappa = 10$  N-m/rad,  $h = 0.1$  m,  $\sigma = 10^3$  1/s,  $\theta_1 = 0.3$  rad,  $\theta_2 = 0.7$  rad, and  $\epsilon = 0.01$  1/s.

## V. CONCLUSIONS

In this paper we introduced a bristle model that exhibits stick-slip friction. The friction force of the bristle model is generated by a frictionless contact between a body and an infinite row of bristles. Each bristle is attached to the

ground through a torsional spring and as the body moves the bristles pivot and counteract its motion. During the motion energy is stored in the torsional springs, so that the bristle model exhibits force-position hysteresis. The stick-slip limit cycles of the bristle model closely resemble the stick-slip limit cycles of the LuGre model. We use this fact to form a hybrid model, that is, a combination of the LuGre and bristle models, that is easier to implement than the bristle model and has the same stick-slip behavior.

## REFERENCES

- [1] C. Makkar, W. E. Dixon, W. G. Sawyer, and G. Hu, "A new continuously differentiable friction model for control systems design," in *IEEE/ASME Int. Conf on Adv. Intell. Mechatronics*, Monterey, CA, 2005, pp. 600–605.
- [2] A. K. Padthe, B. Drincic, J. Oh, D. D. Rigos, S. D. Fassois, and D. S. Bernstein, "Duhem modeling of friction-induced hysteresis: Experimental determination of gearbox stiction," *IEEE Contr. Sys. Mag.*, vol. 28, pp. 90–107, 2008.
- [3] S. H. Park, J. S. Kim, J. J. Choi, and H.-O. Yamazaki, "Modeling and control of adhesion force in railway rolling stocks: Adaptive sliding mode control for the desired wheel slip," *IEEE Contr. Sys. Mag.*, vol. 28, no. 5, pp. 44–58, 2008.
- [4] K. J. Astrom and C. Canudas-De-Wit, "Revisiting the LuGre friction model," *Control Systems Magazine*, vol. 28, no. 6, pp. 101–114, 2008.
- [5] C. Makkar, G. Hu, W. G. Sawyer, and W. E. Dixon, "Lyapunov-based tracking control in presence of uncertain nonlinear parameterizable friction," *IEEE Trans. Autom. Contr.*, vol. 52, no. 10, pp. 1988–1994, 2007.
- [6] H. Olsson, K. J. Åström, C. Canudas de Wit, M. Gafvert, and P. Lischinsky, "Friction models and friction compensation," *European Journal of Control*, vol. 4, no. 3, pp. 176–195, 1998.
- [7] J. Swevers, F. Al-Bender, C. G. Ganseman, and T. Prajogo, "An integrated friction model structure with improved presliding behavior for accurate friction compensation," *IEEE Trans. Autom. Contr.*, vol. 45, no. 4, pp. 675–686, 2000.
- [8] Y. Guo, Z. Qu, Y. Braiman, Z. Zhang, and J. Barhen, "Nanotribology and nanoscale friction: Smooth sliding through feedback control," *IEEE Contr. Sys. Mag.*, vol. 28, no. 6, pp. 92–100, 2008.
- [9] D. M. Rowson, "An analysis of stick-slip motion," *Wear*, vol. 31, pp. 213–218, 1975.
- [10] H. Olsson and K. J. Åström, "Friction generated limit cycles," *IEEE Trans. on Cont. Sys. Tech.*, vol. 9, no. 4, pp. 629–636, 2001.
- [11] R. I. Leine, D. H. V. Campen, and A. D. Kraker, "Stick-slip vibrations induced by alternate friction models," *Nonlin. Dynamics*, vol. 16, pp. 41–54, 1998.
- [12] N. B. Do, A. A. Ferri, and O. A. Bauchau, "Efficient simulation of a dynamic system with LuGre friction," *Journal of Computational and Nonlinear Dynamics*, vol. 2, pp. 281–289, 2007.
- [13] L. C. Bo and D. Pavelescu, "The friction-speed relation and its influence on the critical velocity of stick-slip motion," *Wear*, vol. 82, pp. 277–289, 1982.
- [14] C. J. Radcliffe and S. C. Southward, "A property of stick-slip friction models which promotes limit cycle generation," in *Proc. Amer. Contr. Conf.*, vol. 2, 1990, pp. 1198–1203.
- [15] A. F. D'Souza and A. H. Dweib, "Self-excited vibrations induced by dry friction, part 2: Stability and limit-cycle analysis," *Journal of Sound and Vibration*, vol. 137, no. 2, pp. 177–190, 1990.
- [16] D. A. Haessig and B. Friedland, "On the modeling and simulation of friction," *ASME J. Dyn. Sys. Meas. Contr.*, vol. 113, pp. 354–361, 1991.
- [17] N. E. Dowling, *Mechanical Behavior of Materials: engineering Methods for Deformation, Fracture, and Fatigue*. Englewood Cliffs, NJ: Prentice Hall, 1993.
- [18] F. Al-Bender and J. Swevers, "Characterization of friction force dynamics: Behavior and modeling on micro and macro scales," *IEEE Contr. Sys. Mag.*, vol. 28, no. 6, pp. 82–91, 2008.
- [19] D. S. Bernstein, "Ivory ghost," *IEEE Control Systems Magazine*, vol. 27, no. 5, pp. 16–17, October 2007.
- [20] A. F. Filippov, *Differential Equations with Discontinuous Righthand Sides*. Dordrecht, The Netherlands: Kluwer Academic Publishers, 1988.